



A measurement of $\Delta\Gamma_s$

LHCb collaboration[†]

Abstract

Using a dataset corresponding to 9 fb^{-1} of integrated luminosity collected with the LHCb detector between 2011 and 2018 in proton-proton collisions, the decay-time distributions of the decay modes $B_s^0 \rightarrow J/\psi\eta'$ and $B_s^0 \rightarrow J/\psi\pi^+\pi^-$ are studied. The decay-width difference between the light and heavy mass eigenstates of the B_s^0 meson is measured to be $\Delta\Gamma_s = 0.087 \pm 0.012 \pm 0.009\text{ ps}^{-1}$, where the first uncertainty is statistical and the second systematic.

Submitted to JHEP

© 2023 CERN for the benefit of the LHCb collaboration. CC BY 4.0 licence.

[†]Authors are listed at the end of this paper.

1 Introduction

Measurements of $B_s^0 - \bar{B}_s^0$ mixing parameters are powerful tests of the Standard Model (SM) of particle physics. The B_s^0 and \bar{B}_s^0 flavour eigenstates can be expressed as linear combinations of the heavy (H) and light (L) mass eigenstates. The decay-width difference, $\Delta\Gamma_s = \Gamma_L - \Gamma_H$, is predicted to be in the range $(7.6 - 9.2) \times 10^{-2} \text{ ps}^{-1}$ depending on the choice of the renormalisation scheme [1–4]. Experimentally, the golden channel for the measurement of the $B_s^0 - \bar{B}_s^0$ mixing parameters is the decay $B_s^0 \rightarrow J/\psi\phi$ since it gives a clean experimental signature and is relatively abundant. Measurements of $\Delta\Gamma_s$ using the $B_s^0 \rightarrow J/\psi\phi$ decay have been reported by the ATLAS [5], CMS [6] and LHCb [7] collaborations. Though precise, these measurements are in tension with one another, which results in a large scale factor on the $\Delta\Gamma_s$ uncertainty in the HFLAV average [8]. This has motivated independent measurements in other decay modes such as $B_s^0 \rightarrow J/\psi K^+ K^-$ above the ϕ mass-region [9], and $B_s^0 \rightarrow \psi(2S)\phi$ [10].

The formalism used in this analysis is similar to that proposed in Ref. [11] to measure the B_s^0 mixing phase, ϕ_s . The small value of ϕ_s measured experimentally means that CP -even modes determine the light mass eigenstate lifetime ($\tau_L = 1/\Gamma_L$) while CP -odd modes measure the heavy mass eigenstate lifetime ($\tau_H = 1/\Gamma_H$), to good approximation. Thus, $\Delta\Gamma_s$ can be determined from the decay-width difference between a CP -odd and a CP -even B_s^0 mode.

In this paper, $\Delta\Gamma_s$ is measured from the decay-width difference between the CP -even decay of $B_s^0 \rightarrow J/\psi\eta'$, with subsequent decays $J/\psi \rightarrow \mu^+\mu^-$ and $\eta' \rightarrow \rho^0\gamma$, and the $B_s^0 \rightarrow J/\psi\pi^+\pi^-$ decay mode with the subsequent decay $J/\psi \rightarrow \mu^+\mu^-$. For the latter mode, the dipion mass is required to be within $90 \text{ MeV}/c^2$ of the known $f_0(980)$ mass [12] to select predominantly CP -odd decays [13]. The study is performed using the full dataset collected by the LHCb collaboration in proton-proton (pp) collisions between 2011 and 2018. This corresponds to an integrated luminosity of 9 fb^{-1} collected at centre-of-mass energies of $\sqrt{s} = 7, 8$ and 13 TeV .

The analysis adopts a similar strategy to that used to place a limit on the corresponding parameter in the B^0 -system, $\Delta\Gamma_d$, by the ATLAS collaboration [14]. If CP violation is negligible, the time-dependent decay rate to a CP -eigenstate, f , is

$$\Gamma(B_s^0(t) \rightarrow f) \propto e^{-\Gamma_s t} \left[\cosh\left(\frac{\Delta\Gamma_s t}{2}\right) + \eta_{CP} \sinh\left(\frac{\Delta\Gamma_s t}{2}\right) \right], \quad (1)$$

where $\Gamma_s = (\Gamma_H + \Gamma_L)/2$ and η_{CP} is -1 for a CP -even state and 1 for a CP -odd state. Integrating Eq. 1 over a time bin $[t_1, t_2]$ gives

$$N_L \propto \left[\frac{e^{t(-\frac{\Delta\Gamma_s}{2} - \Gamma_s)}}{\Gamma_s + \frac{\Delta\Gamma_s}{2}} \right]_{t_1}^{t_2}, \quad (2)$$

and

$$N_H \propto \left[\frac{e^{t(\frac{\Delta\Gamma_s}{2} - \Gamma_s)}}{\Gamma_s - \frac{\Delta\Gamma_s}{2}} \right]_{t_1}^{t_2}, \quad (3)$$

where N_L and N_H are the yields of the CP -even and CP -odd modes in that interval. The ratio of the yields in the interval is then

$$R_i = \frac{N_L}{N_H} \propto \frac{[e^{-\Gamma_s t(1+y)}]_{t_1}^{t_2}}{[e^{-\Gamma_s t(1-y)}]_{t_1}^{t_2}} \cdot \frac{(1-y)}{(1+y)}, \quad (4)$$

where $y = \Delta\Gamma_s/2\Gamma_s$. Experimentally, the determination of R_i requires the observed yields $N_{L,H}^{\text{RAW}}$ to be corrected by the relative efficiency in each decay time bin, A_i . By writing

$$R_i = A_i \cdot \frac{N_L^{\text{RAW}}}{N_H^{\text{RAW}}}, \quad (5)$$

$\Delta\Gamma_s$ is determined from a χ^2 minimization of Eq. 4 with $\Delta\Gamma_s$ and an arbitrary normalization factor as free parameters. Though Eq. 4 depends on Γ_s , this dependence is weak and vanishes in the limit of narrow decay-time bins.

The choice of the number of bins and their ranges is made using simulation, with the goal of optimising the sensitivity on $\Delta\Gamma_s$. This results in eight bins (Table 1) with similar yields expected in each. The lower decay-time limit of 0.5 ps is chosen since above this value the time-acceptance is relatively flat. Above 10 ps the expected yield for the $B_s^0 \rightarrow J/\psi\eta'$ decay mode is negligible. Since the last bins are relatively broad, the optimal value of t used to evaluate A_i within a bin needs to be considered [15]. Using pseudoexperiments, the barycentre of the bin calculated using an exponential decay-time model with $\Gamma = \Gamma_s$ is found to minimise the bias on $\Delta\Gamma_s$.

Table 1: Decay-time binning scheme.

Number	Interval [ps]
1	0.5 – 0.7
2	0.7 – 0.9
3	0.9 – 1.2
4	1.2 – 1.5
5	1.5 – 2.0
6	2.0 – 2.5
7	2.5 – 3.5
8	3.5 - 10.0

2 Detector and simulation

The LHCb detector [16, 17] is a single-arm forward spectrometer covering the pseudorapidity range $2 < \eta < 5$, designed for the study of particles containing b or c quarks. It includes a high-precision tracking system consisting of a silicon-strip vertex detector (VELO) surrounding the pp interaction region, a large-area silicon-strip detector (TT) located upstream of a dipole magnet with a bending power of approximately 4 Tm, and three stations of silicon-strip detectors and straw drift tubes placed downstream of the magnet. The tracking system provides a measurement of the momentum, p , of charged particles with a relative uncertainty that varies from 0.5% at low momentum to 1.0% at 200 GeV/ c . Large samples of $J/\psi \rightarrow \mu^+\mu^-$ and $B^+ \rightarrow J/\psi K^+$ decays, collected concurrently with the dataset used in this analysis, are used to calibrate the momentum scale of the spectrometer [18]. The relative uncertainty on the momentum scale is 3×10^{-4} . For b -hadron decay modes such as $B^+ \rightarrow J/\psi K^+$, the mass resolution agrees between data and simulation to better than 10%.

Various charged hadrons are distinguished using information from two ring-imaging Cherenkov (RICH) detectors. In addition, photons, electrons, and hadrons are identified by a calorimeter system consisting of scintillating-pad and preshower detectors, an electromagnetic and a hadronic calorimeter. The calorimeter response is calibrated using samples of $\pi^0 \rightarrow \gamma\gamma$ decays [19]. Muons are identified by a system composed of alternating layers of iron and multiwire proportional chambers.

The online event selection is performed by a trigger, which consists of a hardware stage followed by a two-level software stage [20]. For the Run 2 dataset, the alignment, and calibration of the detector is performed in near real-time such that the results are used in the software trigger [21]. The same alignment and calibration information is propagated to the offline reconstruction, ensuring consistent information between the trigger and offline software. The first stage of the software trigger performs a partial event reconstruction and requires events to have two well-identified oppositely charged muons with an invariant mass larger than $2.7 \text{ GeV}/c^2$ without biasing the lifetime distribution. The second stage performs a full event reconstruction. Events are retained for further processing if they contain a displaced $J/\psi \rightarrow \mu^+\mu^-$ candidate. The J/ψ decay vertex is required to be well separated from each reconstructed primary vertex (PV) of the pp interaction by requiring the distance between the PV and the decay vertex divided by its uncertainty, the decay-length significance, to be greater than three. This introduces a nonuniform efficiency for b -hadron candidates that have a decay time less than $\sim 0.4 \text{ ps}$.

Simulated pp collisions are generated using PYTHIA [22] with a specific LHCb configuration [23]. Decays of hadronic particles are described by EVTGEN [24], in which final-state radiation is generated using PHOTOS [25]. The interaction of the generated particles with the detector, and its response, are implemented using the GEANT4 toolkit [26] as described in Ref. [27]. Several sources of background are also studied using the RapidSim fast simulation package [28].

3 Event selection

The offline selection for both the $B_s^0 \rightarrow J/\psi\eta'$ and $B_s^0 \rightarrow J/\psi\pi^+\pi^-$ modes starts from a pair of oppositely charged particles, identified as muons, that form a common decay vertex. Each muon must have a transverse momentum (p_T) greater than $500 \text{ MeV}/c$ and good track quality. The invariant mass of the $\mu^+\mu^-$ pair is required to be within $\pm 50 \text{ MeV}/c^2$ of the known J/ψ mass [12].

Photon candidates are selected from well-identified neutral clusters reconstructed in the electromagnetic calorimeter that have a transverse energy in excess of 500 MeV . Candidate ρ^0 mesons are reconstructed from pairs of tracks with opposite charge that are identified as pions by the RICH detectors. The invariant mass of the dipion pair is required to be within the range $620\text{--}930 \text{ MeV}/c^2$. To select the $B_s^0 \rightarrow J/\psi\pi^+\pi^-$ decay, pairs of pion candidates with opposite charge are combined in a similar manner. In this case, the invariant mass of the dipion pair is required to be within $90 \text{ MeV}/c^2$ of the world average $f_0(980)$ mass [12] and the scalar sum of the p_T values for the two pions must be greater than $1 \text{ GeV}/c$.

Candidate $\eta' \rightarrow \rho^0\gamma$ decays are formed by combining the selected ρ^0 and γ candidates. The invariant mass of the combination is required to be within $50 \text{ MeV}/c^2$ of the known η' mass [12] and the p_T of the candidate must be larger than $2 \text{ GeV}/c$.

Candidate B_s^0 decays are formed from the selected J/ψ and η' candidates, or dipion pairs. Each B_s^0 candidate is assigned to the PV with the smallest χ_{IP}^2 , where χ_{IP}^2 is defined as the difference in the vertex-fit χ^2 to a given PV reconstructed with and without the candidate tracks being considered. A loose requirement that χ_{IP}^2 is less than 25 effectively reduces combinatorial background. A kinematic vertex fit is applied to the B_s^0 candidates. In this fit, to improve the mass resolution, the J/ψ and η' masses are constrained to their known values [12]. The χ^2 per degree of freedom of this fit is required to be less than 5. As discussed in Sec. 1, only candidates with a decay time in the range 0.5 – 10 ps are selected. As well as removing combinatorial background at low decay times, this defines a region where the acceptance is relatively flat.

For both channels, specific vetoes are applied to remove background from exclusive b -hadron decays. In the case of the $B_s^0 \rightarrow J/\psi\eta'$ decay mode, backgrounds from $B^0 \rightarrow J/\psi\pi^+\pi^-$ and $B_s^0 \rightarrow J/\psi\pi^+\pi^-$ decays combined with a random photon are efficiently suppressed by rejecting $J/\psi\pi^+\pi^-$ combinations with a reconstructed mass greater than 5249 MeV/ c^2 . Background from the decay $B^0 \rightarrow J/\psi K^{*0} (\rightarrow K^+\pi^-)$ is removed by tightening particle identification requirements if either of the two possible reconstructed $J/\psi K^+\pi^-$ masses is within 30 MeV/ c^2 of the known B^0 mass [12]. Finally, background to the $B_s^0 \rightarrow J/\psi\eta'$ mode from the decay $B_s^0 \rightarrow J/\psi\phi (\rightarrow \pi^+\pi^-\pi^0)$ is suppressed by a requirement on the photon helicity angle.

For the $B_s^0 \rightarrow J/\psi\pi^+\pi^-$ decay mode, background from $B^0 \rightarrow J/\psi K^{*0} (\rightarrow K^+\pi^-)$ is suppressed by the dipion mass window requirement and further reduced by the same veto used for the $J/\psi\eta'$ channel. Background from $B^+ \rightarrow J/\psi h^+$ decays, where $h = \pi, K$, is suppressed by rejecting the candidate if any $J/\psi h^+$ combination has a mass within ± 35 MeV/ c^2 of the known B^+ mass [12].

The final step of the selection is to apply a multivariate classifier [29] based on a gradient boosted decision tree (BDTG) [30]. This classifier is trained to distinguish the simulated signal from the data in the background-dominated region where the B-candidate mass is between 5500 and 5650 MeV/ c^2 . In the case of the $B_s^0 \rightarrow J/\psi\pi^+\pi^-$ decay mode, variables related to the b -hadron kinematics, vertex quality and isolation, known to be compatible between data and simulation, are used. For the $B_s^0 \rightarrow J/\psi\eta'$ decay mode, four additional variables, related to kinematics and quality of the photon candidate, are added. The BDTG requirement for the $B_s^0 \rightarrow J/\psi\eta'$ mode is chosen, using pseudoexperiments, to minimise the uncertainty on $\Delta\Gamma_s$. In the case of the $B_s^0 \rightarrow J/\psi\pi^+\pi^-$ mode, since the decay only contains charged particles, the combinatorial background is lower and only a loose requirement on the BDTG response is needed. The chosen requirement keeps 90% of the signal candidates while removing 95% of the background. For both modes, the BDTG requirement does not bias the decay-time distribution. After the full selection, roughly 5% of the events are found to contain more than one candidate. In this case, only one candidate chosen at random is kept.

4 Invariant mass fit

To obtain the yield in each decay-time bin, simultaneous extended unbinned maximum-likelihood fits are performed to the $J/\psi\eta'$ and the $J/\psi\pi^+\pi^-$ invariant mass distributions in the eight decay-time bins described in Sec. 1. Fits are performed separately for the four datasets recorded in 2011&12, 2015&16, 2017, 2018. The invariant mass distributions

with the fit projection overlaid for each dataset are shown in Fig. 1 for the $B_s^0 \rightarrow J/\psi\eta'$ candidates and in Fig. 2 for the $B_s^0 \rightarrow J/\psi\pi^+\pi^-$ candidates.

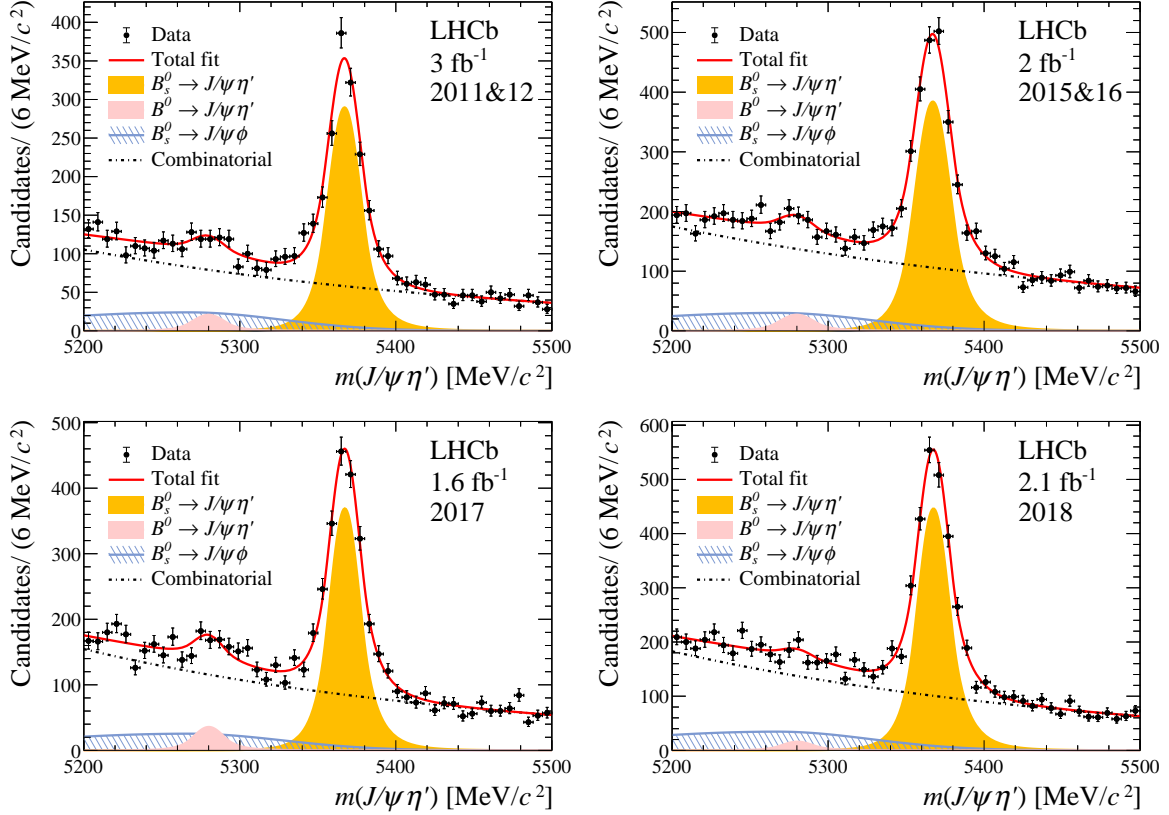


Figure 1: Invariant mass distributions with the fit projection overlaid for the $J/\psi\eta'$ mode for the four datasets. For each dataset the eight time bins are summed.

The fit model for the $J/\psi\eta'$ invariant-mass distribution has four components: the $B_s^0 \rightarrow J/\psi\eta'$ signal, the $B^0 \rightarrow J/\psi\eta'$ decay, the partially reconstructed decay $B_s^0 \rightarrow J/\psi\phi$ with $\phi \rightarrow \pi^+\pi^-\pi^0$, and combinatorial background. The default signal model is chosen to be a double-sided Crystal Ball (DSCB) function. This is a generalization of the Crystal Ball function [31] with power law tails on both sides of the mass peak. In the fit to the data, the DSCB tail parameters are fixed to the values obtained from simulation, while the mean and resolution parameter (σ_r) are left free.

The $B^0 \rightarrow J/\psi\eta'$ decay is modelled using a DSCB shape with the same tail parameters as the B_s^0 component. Since the mass resolution scales with the energy release, Q-value, the resolution parameter for this component is constrained to $s_Q \cdot \sigma_r$, where $s_Q = 0.97 \pm 0.02$. The difference in the positions of the B_s^0 and B^0 mass peaks is also Gaussian-constrained to the known value of $m(B_s^0) - m(B^0) = 87.22 \pm 0.16 \text{ MeV}/c^2$ [12]. The yield of the B^0 component is left free in each decay-time bin since the fraction of B_s^0 and B^0 decays depends on the decay-time.

Partially reconstructed background from the $B_s^0 \rightarrow J/\psi\phi$ decay with $\phi \rightarrow \pi^+\pi^-\pi^0$ is modelled with a bifurcated Gaussian function. In the fit to the data, the shape parameters are fixed to the values obtained from simulation while the relative fraction compared to the signal mode, f_ϕ , is left free. The combinatorial background component is modelled by

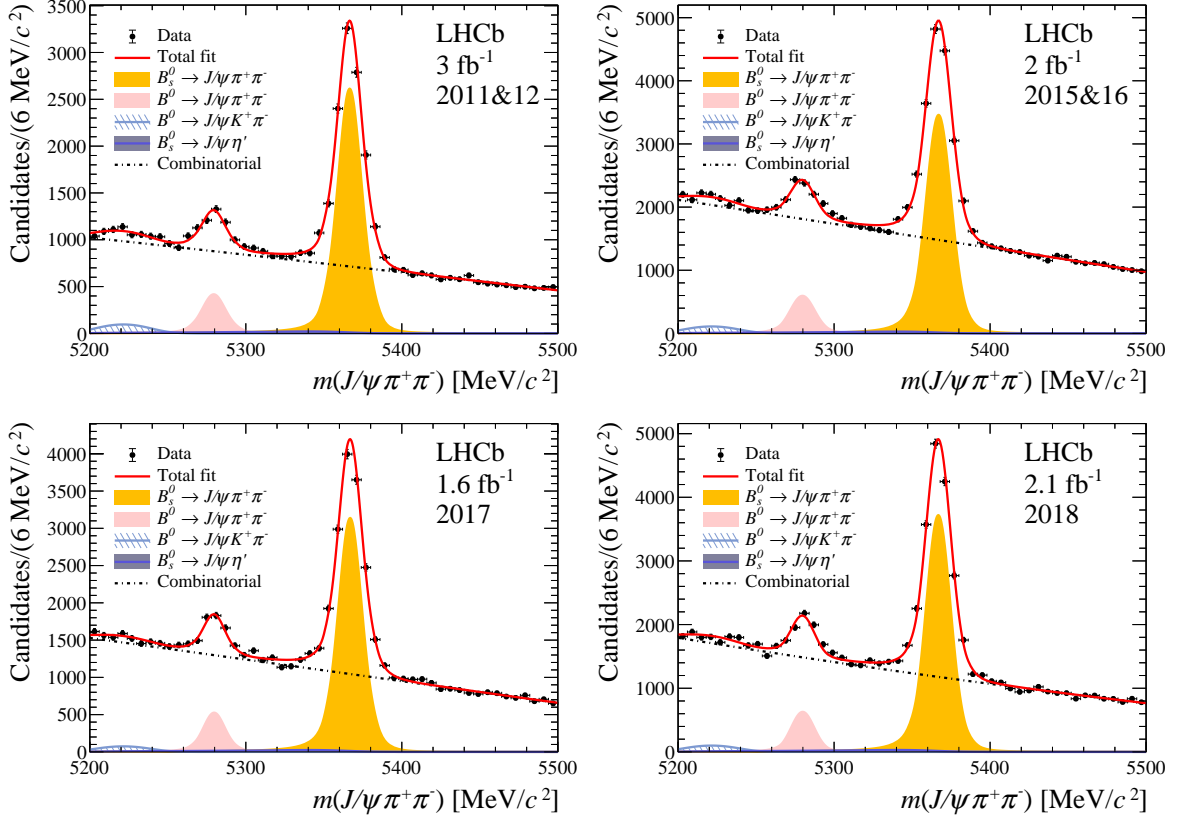


Figure 2: Invariant mass distributions with the fit projection overlaid for the $J/\psi\pi^+\pi^-$ mode for the four datasets. For each dataset the eight time bins are summed.

an exponential function, with the slope allowed to float independently in each of the eight decay-time bins.

The $J/\psi\pi^+\pi^-$ invariant-mass fit model has five components: the $B_s^0 \rightarrow J/\psi\pi^+\pi^-$ signal, the $B^0 \rightarrow J/\psi\pi^+\pi^-$ decay, the misreconstructed $B^0 \rightarrow J/\psi K^+\pi^-$ decay, $B_s^0 \rightarrow J/\psi\eta'$ decays with $\eta' \rightarrow \pi^+\pi^-\gamma$, and combinatorial background. The invariant mass distribution of the $B_s^0 \rightarrow J/\psi\pi^+\pi^-$ decay is well described by the sum of two DSCB functions with common mean and tail parameters. In the fit to the data, the tail parameters are fixed to the values obtained from simulation. Each of the two resolution parameters obtained from the simulation are multiplied by a scale-factor that varies freely in the fit. The $B^0 \rightarrow J/\psi\pi^+\pi^-$ decay is dominated by an intermediate ρ^0 meson and is suppressed by the requirement that the dipion mass is within $90 \text{ MeV}/c^2$ of the known mass of the $f_0(980)$ resonance. The remaining background from this source is modelled with the sum of two DSCB functions with the same tail and fraction parameters as for the $B_s^0 \rightarrow J/\psi\pi^+\pi^-$ decay. The position of the peak is Gaussian-constrained relative to the B_s^0 and the mass resolution is constrained to the B_s^0 mode assuming Q-value scaling.

The decay $B^0 \rightarrow J/\psi K^+\pi^-$ is suppressed using the veto explained in Sec. 3. The shape of the remaining background from this source is modelled using a histogram template obtained from the RapidSim simulation which is convolved with the detector resolution. The size of this component is estimated by studying the $J/\psi K^+\pi^-$ invariant mass distribution in data. Using these studies, the fraction of this component is constrained

relative to the signal to be 0.01 ± 0.1 .

Background from the partially reconstructed decay $B_s^0 \rightarrow J/\psi\eta'$ with $\eta' \rightarrow \pi^+\pi^-\gamma$ is modelled using a histogram template from the RapidSim simulation which is convolved with the detector resolution. The relative yield of the component to the signal decay is constrained to be $f_{\eta'} = 0.6 \pm 0.9\%$ using the known branching fractions and the relative efficiency obtained from the simulation. Finally, by combining pairs of same-sign pion candidates with selected J/ψ candidates, the combinatorial background component is found to be well modelled by a second-order Chebychev polynomial. Based on the same-sign fits, in order to minimise the free parameters in the simultaneous fit to the data, the second-order parameter of this function is shared between the decay-time bins, while the first order parameter is left free and allowed to vary in each bin.

5 Decay-time acceptance

Due to the requirements made in the trigger and offline selection, the acceptance of the detector varies with decay time. At low decay times, the decay-length significance requirement removes events, while at high decay time, inefficiencies are introduced by the requirement on the candidate χ_{IP}^2 and the VELO track reconstruction [32]. The simulation is used to verify that the decay-time acceptance largely cancels due to the similarity of the two decays and their selections. The remaining relative acceptance correction is found to be well described by the form $A_r(t) = 1 - \beta t$, using the simulation. The result of a fit to the simulation of this form is used to generate the acceptance correction, A_i , for each bin by evaluating $A_r(t)$ at the bin barycentre. The largest relative acceptance correction (1.18) is found in the last bin of the 2011&12 dataset since the size of the VELO tracking-efficiency correction is large [33] for each mode, and thus it does not cancel in A_i . For the other datasets, improvements to the VELO tracking algorithm lead to a smaller relative acceptance correction of 1.03 or less. The overall effect of the relative acceptance correction is small. If it were ignored entirely, the central value of $\Delta\Gamma_s$ would change by half the statistical uncertainty. As part of the systematic studies, alternative functional forms and choices to evaluate the acceptance are considered. Another approach, used as a cross-check, is to assume the acceptance is flat within a decay-time bin. In this case, the relative acceptance from the simulation is extracted directly in the eight decay-time bins.

6 Results and systematic uncertainties

The yields of the $B_s^0 \rightarrow J/\psi\eta'$ and $B_s^0 \rightarrow J/\psi\pi^+\pi^-$ decay are extracted from the extended unbinned simultaneous maximum-likelihood fit to the eight decay-time bins described in Sec. 4. The ratio of yields in each bin is corrected by the corresponding relative decay-time acceptance, and the χ^2 fit described in Sec. 1 is performed. Figure 3 shows the fit result for each dataset. The resulting values of $\Delta\Gamma_s$ are summarized in Table 2. The weighted average of the results is $\Delta\Gamma_s = 0.087 \pm 0.012 \text{ ps}^{-1}$ where the uncertainty is statistical.

Systematic uncertainties related to the knowledge of the detector acceptance largely cancel in A_i . The uncertainty from the finite size of the available simulation samples is estimated by resampling the covariance matrix of the fit used to obtain β , running the fit procedure and calculating the weighted average of the four datasets. This results in a systematic uncertainty of 4.6 ns^{-1} . In the baseline fit, a linear model is used to determine

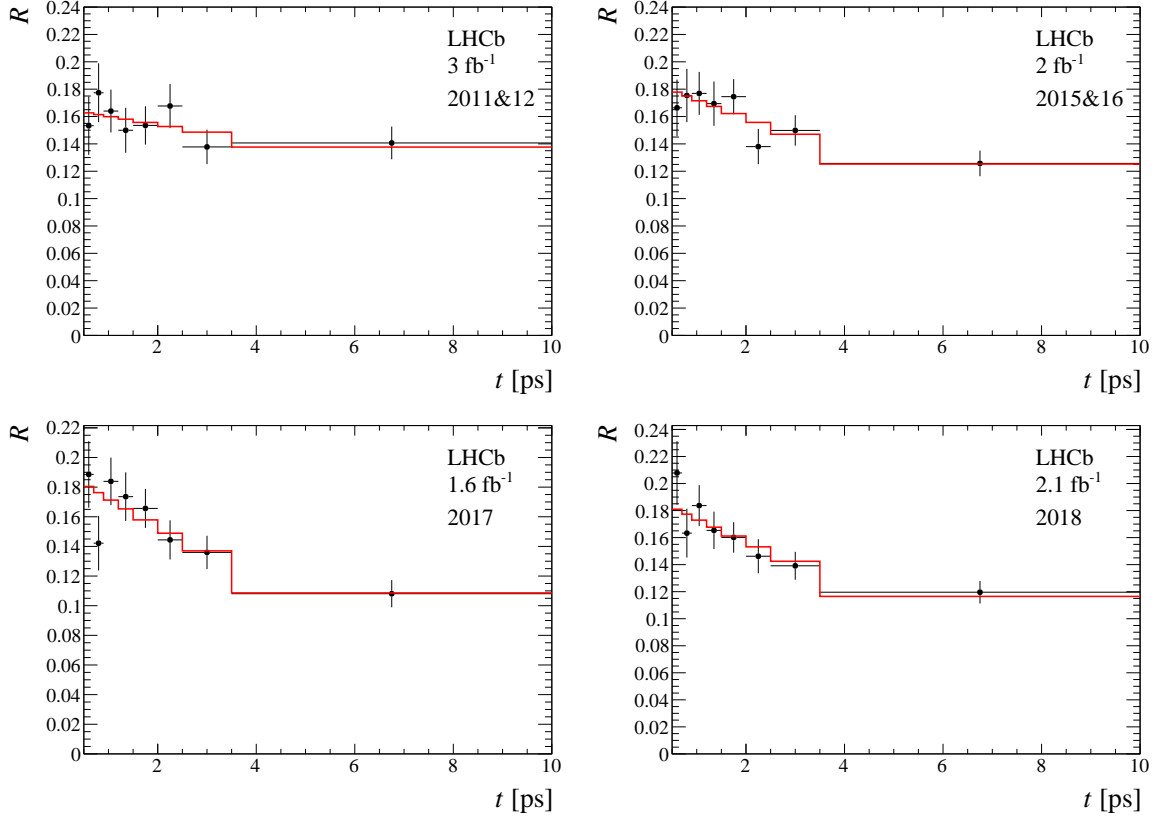


Figure 3: Measurements of R for the four datasets. The red line for each plot shows the result of the fit described in the text.

Table 2: Values of $\Delta\Gamma_s$ and the χ^2 probability obtained from the fits to R for the four datasets. The uncertainties are statistical.

Dataset	$\Delta\Gamma_s$ [ps^{-1}]	$P(\chi^2)$
2011&12	0.039 ± 0.026	0.83
2015&16	0.081 ± 0.022	0.77
2017	0.117 ± 0.024	0.57
2018	0.102 ± 0.021	0.78

A_i . To estimate the uncertainty due to this choice, a parabolic model and a histogram-based approach are considered. Based on these studies, an uncertainty of 3.0 ns^{-1} is assigned. For the 2011&12 dataset, where the acceptance corrections due to the trigger and selection are largest, additional data-driven checks of the acceptance ratio are made using the methods described in Ref. [33]. Though the individual acceptance correction for each mode changes, A_i is not significantly affected, and no further uncertainty is assigned.

The correctness of the fit procedure has been extensively verified using pseudoexperiments. The largest bias found in those tests arises from the choice of the decay-time value used to evaluate the acceptance correction. Based upon those studies, a 0.3 ns^{-1} uncertainty is assigned.

Several uncertainties arise from the limited knowledge of physics inputs to the fit.

Table 3: Systematic uncertainties on the measurement of $\Delta\Gamma_s$.

Source	Value [ns^{-1}]
Simulation sample size	4.6
Acceptance model	3.0
Bin centre method	0.3
CP violation	0.1
Γ_s	0.1
$J/\psi\eta'$ background model	6.9
$J/\psi\pi^+\pi^-$ background model	0.8
Total	8.9

The method assumes that ϕ_s is zero. Experimentally, the current world average is $\phi_s = -0.049 \pm 0.019$ rad [8]. Based upon pseudoexperiments, a systematic uncertainty of 0.1 ns^{-1} is assigned to allow for a non-zero value of ϕ_s . The analysis uses $B_s^0 \rightarrow J/\psi\pi^+\pi^-$ decays with a dipion mass within $90 \text{ MeV}/c^2$ of the known $f_0(980)$ mass, which are predominantly CP -odd. The angular analysis in Ref. [34] limits the size of the CP -even component in this dipion mass region to be less than 0.6% at 95% confidence level. Including a 0.6% CP -even component in the generation of pseudoexperiments and ignoring it in the fit results in a negligible bias. The default fit uses the current world average, $\Gamma_s = 0.6628 \pm 0.0035 \text{ ps}^{-1}$ [8], as input. Varying Γ_s within its uncertainty results in a 0.1 ns^{-1} uncertainty on $\Delta\Gamma_s$.

Another source of uncertainty arises from the modelling of the signal and background components in the mass fits used to determine the yields. Using alternative models to describe the signal distribution gives consistent results to the default fit. The impact of the background model is evaluated by varying the assumptions related to the modelling of the short-lived combinatorial and long-lived partially reconstructed components. The only significant variation is found to come from the combinatorial background model. For the $B_s^0 \rightarrow J/\psi\eta'$ mode, as an alternative to the baseline exponential model, a first-order Chebychev function is considered. Using the fit results obtained for each bin, pseudoexperiments are generated with the default model, and then fit with the alternative background model. A bias of $6.9 \pm 0.1 \text{ ns}^{-1}$ is found for the $B_s^0 \rightarrow J/\psi\eta'$ mode and assigned as a systematic uncertainty. For the $B_s^0 \rightarrow J/\psi\pi^+\pi^-$ mode, generating pseudoexperiments with a first-order Chebychev polynomial and then fitting with a second-order (and vice versa) results in a bias of $0.8 \pm 0.1 \text{ ns}^{-1}$, which is assigned as the systematic uncertainty due to the background model.

The systematic uncertainties are summarized in Table 3. Adding them in quadrature leads to a total systematic uncertainty of 8.9 ns^{-1} . The stability of the result is tested by comparing the results for the four datasets (Fig. 4). The χ^2 probability for the four measurements, accounting for the statistical uncertainty and the uncorrelated part of the systematic uncertainty, is 12% indicating that the four values are in good agreement.

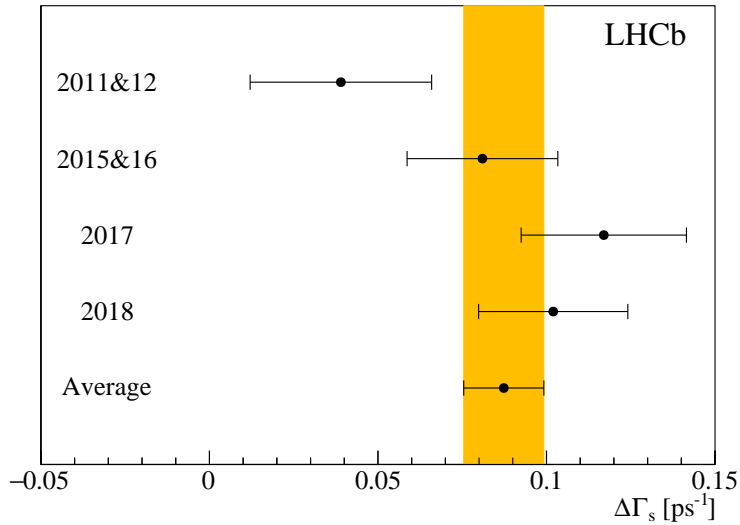


Figure 4: Measurement of $\Delta\Gamma_s$ for the four datasets and their weighted average. The orange band is the 1σ error band.

7 Summary

Using the full LHCb pp collision dataset collected between 2011 and 2018, the $B_s^0 \rightarrow J/\psi\eta'$ and $B_s^0 \rightarrow J/\psi\pi^+\pi^-$ decay modes are used to measure the decay-width difference

$$\Delta\Gamma_s = 0.087 \pm 0.012 \pm 0.009 \text{ ps}^{-1},$$

where the first uncertainty is statistical and the second systematic. This is the first time-dependent measurement using the $B_s^0 \rightarrow J/\psi\eta'$ decay mode. The value is in agreement with the HFLAV average, $\Delta\Gamma_s = 0.074 \pm 0.006 \text{ ps}^{-1}$ [8], determined from the time-dependent angular analyses of the $B_s^0 \rightarrow J/\psi\phi$ decay mode where the initial flavour of the state is tagged. It also agrees with the HFLAV average, $\Delta\Gamma_s = 0.083 \pm 0.005 \text{ ps}^{-1}$ [8], which includes constraints from other untagged effective lifetime measurements. The alternative approach to determine $\Delta\Gamma_s$ presented in this paper may help to resolve the observed tensions between the measurements made by the LHC collaborations in the $B_s^0 \rightarrow J/\psi\phi$ mode.

Acknowledgements

We express our gratitude to our colleagues in the CERN accelerator departments for the excellent performance of the LHC. We thank the technical and administrative staff at the LHCb institutes. We acknowledge support from CERN and from the national agencies: CAPES, CNPq, FAPERJ and FINEP (Brazil); MOST and NSFC (China); CNRS/IN2P3 (France); BMBF, DFG and MPG (Germany); INFN (Italy); NWO (Netherlands); MNiSW and NCN (Poland); MCID/IFA (Romania); MICINN (Spain); SNSF and SER (Switzerland); NASU (Ukraine); STFC (United Kingdom); DOE NP and NSF (USA). We acknowledge the computing resources that are provided by CERN, IN2P3 (France), KIT and DESY (Germany), INFN (Italy), SURF (Netherlands), PIC (Spain), GridPP (United Kingdom), CSCS (Switzerland), IFIN-HH (Romania), CBPF (Brazil), Polish WLCG (Poland) and NERSC (USA). We are indebted to the communities behind the multiple open-source software packages on which we depend. Individual groups or members have received support from ARC and ARDC (Australia); Key Research Program of Frontier Sciences of CAS, CAS PIFI, CAS CCEPP, Fundamental Research Funds for the Central Universities, and Sci. & Tech. Program of Guangzhou (China); Minciencias (Colombia); EPLANET, Marie Skłodowska-Curie Actions, ERC and NextGenerationEU (European Union); A*MIDEX, ANR, IPhU and Labex P2IO, and Région Auvergne-Rhône-Alpes (France); AvH Foundation (Germany); ICSC (Italy); GVA, XuntaGal, GENCAT, Inditex, InTalent and Prog. Atracción Talento, CM (Spain); SRC (Sweden); the Leverhulme Trust, the Royal Society and UKRI (United Kingdom).

References

- [1] H. M. Asatrian *et al.*, *Penguin contribution to the width difference and asymmetry in mixing*, Phys. Rev. **D102** (2020) 033007, [arXiv:2006.13227](#).
- [2] HPQCD collaboration, C. T. H. Davies *et al.*, *Lattice QCD matrix elements for the $B_s^0 - \bar{B}_s^0$ width difference*, Phys. Rev. Lett. **124** (2020) 082001, [arXiv:1910.00970](#).
- [3] A. Lenz and G. Tetlalmatzi-Xolocotzi, *Model-independent bounds on new physics effects*, JHEP **07** (2020) 177, [arXiv:1912.07621](#).
- [4] M. Gerlach *et al.*, *The width difference in $B - \bar{B}$ mixing at order α_s and beyond*, JHEP **04** (2022) 006, [arXiv:2202.12305](#).
- [5] ATLAS collaboration, G. Aad *et al.*, *Measurement of the CP-violating phase ϕ_s in $B_s^0 \rightarrow J/\psi\phi$ decays in ATLAS at 13 TeV*, Eur. Phys. J. **C81** (2021) 342, [arXiv:2001.07115](#).
- [6] CMS collaboration, A. M. Sirunyan *et al.*, *Measurement of the CP-violating phase ϕ_s in the $B_s^0 \rightarrow J/\psi\phi \rightarrow \mu^+\mu^-K^+K^-$ channel in proton-proton collisions at $\sqrt{s} = 13$ TeV*, Phys. Lett. **B816** (2021) 136188, [arXiv:2007.02434](#).
- [7] LHCb collaboration, R. Aaij *et al.*, *Improved measurement of CP violation parameters in $B_s^0 \rightarrow J/\psi K^+K^-$ decays in the vicinity of the $\phi(1020)$ resonance*, [arXiv:2308.01468](#), submitted to Phys. Rev. Lett.

- [8] Y. Amhis *et al.*, *Averages of b -hadron, c -hadron, and τ -lepton properties as of 2021*, Phys. Rev. **D107** (2023) 052008, [arXiv:2206.07501](https://arxiv.org/abs/2206.07501), updated results and plots available at <https://hflav.web.cern.ch>.
- [9] LHCb collaboration, R. Aaij *et al.*, *Resonances and CP-violation in B_s^0 and $\bar{B}_s^0 \rightarrow J/\psi K^+ K^-$ decays in the mass region above the $\phi(1020)$* , JHEP **08** (2017) 037, [arXiv:1704.08217](https://arxiv.org/abs/1704.08217).
- [10] LHCb collaboration, R. Aaij *et al.*, *Measurement of the CP violating phase and decay-width difference in $B_s^0 \rightarrow \psi(2S)\phi$ decays*, Phys. Lett. **B762** (2016) 253, [arXiv:1608.04855](https://arxiv.org/abs/1608.04855).
- [11] R. Fleischer and R. Knegjens, *Effective lifetime of B_s decays and B_s^0 - \bar{B}_s^0 mixing parameters*, Eur. Phys. J. **C71** (2011) 1789, [arXiv:1109.5115](https://arxiv.org/abs/1109.5115).
- [12] Particle Data Group, R. L. Workman *et al.*, *Review of particle physics*, Prog. Theor. Exp. Phys. **2022** (2022) 083C01.
- [13] LHCb collaboration, R. Aaij *et al.*, *Measurement of resonant and CP components in $\bar{B}_s^0 \rightarrow J/\psi \pi^+ \pi^-$ decays*, Phys. Rev. **D89** (2014) 092006, [arXiv:1402.6248](https://arxiv.org/abs/1402.6248).
- [14] ATLAS collaboration, M. Aaboud *et al.*, *Measurement of the relative width difference of the B^0 - \bar{B}^0 system with the ATLAS detector*, JHEP **06** (2016) 081, [arXiv:1605.07485](https://arxiv.org/abs/1605.07485).
- [15] G. D. Lafferty and T. R. Wyatt, *Where to stick your data points: The treatment of measurements within wide bins*, Nucl. Instrum. Meth. **A355** (1995) 541.
- [16] A. A. Alves Jr. *et al.*, *Performance of the LHCb muon system*, JINST **8** (2013) P02022, [arXiv:1211.1346](https://arxiv.org/abs/1211.1346).
- [17] LHCb collaboration, R. Aaij *et al.*, *LHCb detector performance*, Int. J. Mod. Phys. **A30** (2015) 1530022, [arXiv:1412.6352](https://arxiv.org/abs/1412.6352).
- [18] LHCb collaboration, R. Aaij *et al.*, *Precision measurement of D meson mass differences*, JHEP **06** (2013) 065, [arXiv:1304.6865](https://arxiv.org/abs/1304.6865).
- [19] C. Abellan Beteta *et al.*, *Calibration and performance of the LHCb calorimeters in Run 1 and 2 at the LHC*, [arXiv:2008.11556](https://arxiv.org/abs/2008.11556), submitted to JINST.
- [20] R. Aaij *et al.*, *Performance of the LHCb trigger and full real-time reconstruction in Run 2 of the LHC*, JINST **14** (2019) P04013, [arXiv:1812.10790](https://arxiv.org/abs/1812.10790).
- [21] S. Borghi, *Novel real-time alignment and calibration of the LHCb detector and its performance*, Nucl. Instrum. Meth. **A845** (2017) 560.
- [22] T. Sjöstrand, S. Mrenna, and P. Skands, *A brief introduction to PYTHIA 8.1*, Comput. Phys. Commun. **178** (2008) 852, [arXiv:0710.3820](https://arxiv.org/abs/0710.3820).
- [23] I. Belyaev *et al.*, *Handling of the generation of primary events in Gauss, the LHCb simulation framework*, J. Phys. Conf. Ser. **331** (2011) 032047.

- [24] D. J. Lange, *The EvtGen particle decay simulation package*, Nucl. Instrum. Meth. **A462** (2001) 152.
- [25] P. Golonka and Z. Was, *PHOTOS Monte Carlo: A precision tool for QED corrections in Z and W decays*, Eur. Phys. J. **C45** (2006) 97, [arXiv:hep-ph/0506026](#).
- [26] Geant4 collaboration, J. Allison *et al.*, *Geant4 developments and applications*, IEEE Trans. Nucl. Sci. **53** (2006) 270; Geant4 collaboration, S. Agostinelli *et al.*, *Geant4: A simulation toolkit*, Nucl. Instrum. Meth. **A506** (2003) 250.
- [27] M. Clemencic *et al.*, *The LHCb simulation application, Gauss: Design, evolution and experience*, J. Phys. Conf. Ser. **331** (2011) 032023.
- [28] G. A. Cowan, D. C. Craik, and M. D. Needham, *RapidSim: an application for the fast simulation of heavy-quark hadron decays*, Comput. Phys. Commun. **214** (2017) 239, [arXiv:1612.07489](#).
- [29] H. Voss, A. Hoecker, J. Stelzer, and F. Tegenfeldt, *TMVA - Toolkit for Multivariate Data Analysis with ROOT*, PoS **ACAT** (2007) 040; A. Hoecker *et al.*, *TMVA 4 — Toolkit for Multivariate Data Analysis with ROOT. Users Guide.*, [arXiv:physics/0703039](#).
- [30] B. P. Roe *et al.*, *Boosted decision trees as an alternative to artificial neural networks for particle identification*, Nucl. Instrum. Meth. **A543** (2005) 577, [arXiv:physics/0408124](#).
- [31] T. Skwarnicki, *A study of the radiative cascade transitions between the Upsilon-prime and Upsilon resonances*, PhD thesis, Institute of Nuclear Physics, Krakow, 1986, DESY-F31-86-02.
- [32] LHCb collaboration, R. Aaij *et al.*, *Measurement of τ_L using the $B_s^0 \rightarrow J/\psi\eta$ decay mode*, Eur. Phys. J. **C83** (2023) 629, [arXiv:2206.03088](#).
- [33] LHCb collaboration, R. Aaij *et al.*, *Measurements of the B^+ , B^0 , B_s^0 meson and Λ_b^0 baryon lifetimes*, JHEP **04** (2014) 114, [arXiv:1402.2554](#).
- [34] LHCb collaboration, R. Aaij *et al.*, *Analysis of the resonant components in $\bar{B}_s^0 \rightarrow J/\psi\pi^+\pi^-$* , Phys. Rev. **D86** (2012) 052006, [arXiv:1204.5643](#).

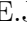






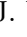

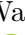










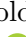
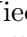




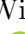
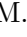
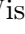


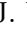


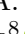


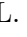
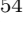

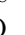

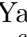

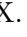

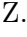
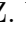
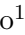
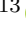

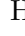
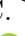
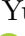
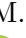

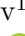



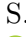



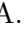


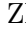
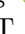
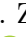



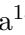






LHCb collaboration

R. Aaij³⁵ , A.S.W. Abdelmotteleb⁵⁴ , C. Abellan Beteta⁴⁸ , F. Abudinén⁵⁴ ,
T. Ackernley⁵⁸ , B. Adeva⁴⁴ , M. Adinolfi⁵² , P. Adlarson⁷⁸ , H. Afsharnia¹¹ ,
C. Agapopoulou⁴⁶ , C.A. Aidala⁷⁹ , Z. Ajaltouni¹¹ , S. Akar⁶³ , K. Akiba³⁵ ,
P. Albicocco²⁵ , J. Albrecht¹⁷ , F. Alessio⁴⁶ , M. Alexander⁵⁷ , A. Alfonso Albero⁴³ ,
Z. Aliouche⁶⁰ , P. Alvarez Cartelle⁵³ , R. Amalric¹⁵ , S. Amato³ , J.L. Amey⁵² ,
Y. Amhis^{13,46} , L. An⁶ , L. Anderlini²⁴ , M. Andersson⁴⁸ , A. Andreianov⁴¹ ,
P. Andreola⁴⁸ , M. Andreotti²³ , D. Andreou⁶⁶ , A. A. Anelli^{28,n} , D. Ao⁷ ,
F. Archilli^{34,t} , S. Arguedas Cuendis⁹ , A. Artamonov⁴¹ , M. Artuso⁶⁶ , E. Aslanides¹² ,
M. Atzeni⁶² , B. Audurier¹⁴ , D. Bacher⁶¹ , I. Bachiller Perea¹⁰ , S. Bachmann¹⁹ ,
M. Bachmayer⁴⁷ , J.J. Back⁵⁴ , A. Bailly-reyre¹⁵ , P. Baladron Rodriguez⁴⁴ ,
V. Balagura¹⁴ , W. Baldini²³ , J. Baptista de Souza Leite² , M. Barbetti^{24,k} , I.
R. Barbosa⁶⁷ , R.J. Barlow⁶⁰ , S. Barsuk¹³ , W. Barter⁵⁶ , M. Bartolini⁵³ ,
F. Baryshnikov⁴¹ , J.M. Basels¹⁶ , G. Bassi^{32,q} , B. Batsukh⁵ , A. Battig¹⁷ ,
A. Bay⁴⁷ , A. Beck⁵⁴ , M. Becker¹⁷ , F. Bedeschi³² , I.B. Bediaga² , A. Beiter⁶⁶ ,
S. Belin⁴⁴ , V. Bellee⁴⁸ , K. Belous⁴¹ , I. Belov²⁶ , I. Belyaev⁴¹ , G. Benane¹² ,
G. Bencivenni²⁵ , E. Ben-Haim¹⁵ , A. Berezhnoy⁴¹ , R. Bernet⁴⁸ , S. Bernet Andres⁴² ,
H.C. Bernstein⁶⁶ , C. Bertella⁶⁰ , A. Bertolin³⁰ , C. Betancourt⁴⁸ , F. Betti⁵⁶ , J.
Bex⁵³ , I.a. Bezshyiko⁴⁸ , J. Bhom³⁸ , M.S. Bieker¹⁷ , N.V. Biesuz²³ , P. Billoir¹⁵ ,
A. Biolchini³⁵ , M. Birch⁵⁹ , F.C.R. Bishop¹⁰ , A. Bitadze⁶⁰ , A. Bizzeti ,
M.P. Blago⁵³ , T. Blake⁵⁴ , F. Blanc⁴⁷ , J.E. Blank¹⁷ , S. Blusk⁶⁶ , D. Bobulska⁵⁷ ,
V. Bocharnikov⁴¹ , J.A. Boelhaue¹⁷ , O. Boente Garcia¹⁴ , T. Boettcher⁶³ , A.
Bohare⁵⁶ , A. Boldyrev⁴¹ , C.S. Bolognani⁷⁶ , R. Bolzonella^{23,j} , N. Bondar⁴¹ ,
F. Borgato^{30,46} , S. Borghi⁶⁰ , M. Borsato^{28,n} , J.T. Borsuk³⁸ , S.A. Bouchiba⁴⁷ ,
T.J.V. Bowcock⁵⁸ , A. Boyer⁴⁶ , C. Bozzi²³ , M.J. Bradley⁵⁹ , S. Braun⁶⁴ ,
A. Brea Rodriguez⁴⁴ , N. Breer¹⁷ , J. Brodzicka³⁸ , A. Brossa Gonzalo⁴⁴ , J. Brown⁵⁸ ,
D. Brundu²⁹ , A. Buonauro⁴⁸ , L. Buonincontri³⁰ , A.T. Burke⁶⁰ , C. Burr⁴⁶ ,
A. Bursche⁶⁹ , A. Butkevich⁴¹ , J.S. Butter⁵³ , J. Buytaert⁴⁶ , W. Byczynski⁴⁶ ,
S. Cadeddu²⁹ , H. Cai⁷¹ , R. Calabrese^{23,j} , L. Calefice¹⁷ , S. Cali²⁵ , M. Calvi^{28,n} ,
M. Calvo Gomez⁴² , J. Cambon Bouzas⁴⁴ , P. Campana²⁵ , D.H. Campora Perez⁷⁶ ,
A.F. Campoverde Quezada⁷ , S. Capelli^{28,n} , L. Capriotti²³ , R. Caravaca-Mora⁹ ,
A. Carbone^{22,h} , L. Carcedo Salgado⁴⁴ , R. Cardinale^{26,l} , A. Cardini²⁹ , P. Carniti^{28,n} ,
L. Carus¹⁹ , A. Casais Vidal⁶² , R. Caspary¹⁹ , G. Casse⁵⁸ , J. Castro Godinez⁹ ,
M. Cattaneo⁴⁶ , G. Cavallero²³ , V. Cavallini^{23,j} , S. Celani⁴⁷ , J. Cerasoli¹² ,
D. Cervenkov⁶¹ , S. Cesare^{27,m} , A.J. Chadwick⁵⁸ , I. Chahrour⁷⁹ , M. Charles¹⁵ ,
Ph. Charpentier⁴⁶ , C.A. Chavez Barajas⁵⁸ , M. Chefdeville¹⁰ , C. Chen¹² , S. Chen⁵ ,
A. Chernov³⁸ , S. Chernyshenko⁵⁰ , V. Chobanova^{44,x} , S. Cholak⁴⁷ , M. Chruszcz³⁸ ,
A. Chubykin⁴¹ , V. Chulikov⁴¹ , P. Ciambone²⁵ , M.F. Cicala⁵⁴ , X. Cid Vidal⁴⁴ ,
G. Ciezarek⁴⁶ , P. Cifra⁴⁶ , P.E.L. Clarke⁵⁶ , M. Clemencic⁴⁶ , H.V. Cliff⁵³ ,
J. Closier⁴⁶ , J.L. Cobbledick⁶⁰ , C. Cocha Toapaxi¹⁹ , V. Coco⁴⁶ , J. Cogan¹² ,
E. Cogneras¹¹ , L. Cojocariu⁴⁰ , P. Collins⁴⁶ , T. Colombo⁴⁶ , A. Comerma-Montells⁴³ ,
L. Congedo²¹ , A. Contu²⁹ , N. Cooke⁵⁷ , I. Corredoira⁴⁴ , A. Correia¹⁵ , G. Corti⁴⁶ ,
J.J. Cottee Meldrum⁵² , B. Couturier⁴⁶ , D.C. Craik⁴⁸ , M. Cruz Torres^{2,f} , R. Currie⁵⁶ ,
C.L. Da Silva⁶⁵ , S. Dadabaev⁴¹ , L. Dai⁶⁸ , X. Dai⁶ , E. Dall'Occo¹⁷ , J. Dalseno⁴⁴ ,
C. D'Ambrosio⁴⁶ , J. Daniel¹¹ , A. Danilina⁴¹ , P. d'Argent²¹ , A. Davidson⁵⁴ ,
J.E. Davies⁶⁰ , A. Davis⁶⁰ , O. De Aguiar Francisco⁶⁰ , C. De Angelis^{29,i} , J. de Boer³⁵ ,
K. De Bruyn⁷⁵ , S. De Capua⁶⁰ , M. De Cian¹⁹ , U. De Freitas Carneiro Da Graca^{2,b} ,
E. De Lucia²⁵ , J.M. De Miranda² , L. De Paula³ , M. De Serio^{21,g} , D. De Simone⁴⁸ ,
P. De Simone²⁵ , F. De Vellis¹⁷ , J.A. de Vries⁷⁶ , F. Debernardis^{21,g} , D. Decamp¹⁰ ,

V. Dedu¹² , L. Del Buono¹⁵ , B. Delaney⁶² , H.-P. Dembinski¹⁷ , J. Deng⁸ ,
 V. Denysenko⁴⁸ , O. Deschamps¹¹ , F. Dettori^{29,i} , B. Dey⁷⁴ , P. Di Nezza²⁵ ,
 I. Diachkov⁴¹ , S. Didenko⁴¹ , S. Ding⁶⁶ , V. Dobishuk⁵⁰ , A. D. Docheva⁵⁷ ,
 A. Dolmatov⁴¹ , C. Dong⁴ , A.M. Donohoe²⁰ , F. Dordei²⁹ , A.C. dos Reis² ,
 L. Douglas⁵⁷ , A.G. Downes¹⁰ , W. Duan⁶⁹ , P. Duda⁷⁷ , M.W. Dudek³⁸ , L. Dufour⁴⁶ ,
 V. Duk³¹ , P. Durante⁴⁶ , M. M. Duras⁷⁷ , J.M. Durham⁶⁵ , D. Dutta⁶⁰ ,
 A. Dziurda³⁸ , A. Dzyuba⁴¹ , S. Easo^{55,46} , E. Eckstein⁷³ , U. Egede¹ , A. Egorychev⁴¹ ,
 V. Egorychev⁴¹ , C. Eirea Orro⁴⁴ , S. Eisenhardt⁵⁶ , E. Ejopu⁶⁰ , S. Ek-In⁴⁷ ,
 L. Eklund⁷⁸ , M. Elashri⁶³ , J. Ellbracht¹⁷ , S. Ely⁵⁹ , A. Ene⁴⁰ , E. Epple⁶³ ,
 S. Escher¹⁶ , J. Eschle⁴⁸ , S. Esen⁴⁸ , T. Evans⁶⁰ , F. Fabiano^{29,i,46} , L.N. Falcao² ,
 Y. Fan⁷ , B. Fang^{71,13} , L. Fantini^{31,p} , M. Faria⁴⁷ , K. Farmer⁵⁶ , D. Fazzini^{28,n} ,
 L. Felkowski⁷⁷ , M. Feng^{5,7} , M. Feo⁴⁶ , M. Fernandez Gomez⁴⁴ , A.D. Fernez⁶⁴ ,
 F. Ferrari²² , F. Ferreira Rodrigues³ , S. Ferreres Sole³⁵ , M. Ferrillo⁴⁸ ,
 M. Ferro-Luzzi⁴⁶ , S. Filippov⁴¹ , R.A. Fini²¹ , M. Fiorini^{23,j} , M. Firlej³⁷ ,
 K.M. Fischer⁶¹ , D.S. Fitzgerald⁷⁹ , C. Fitzpatrick⁶⁰ , T. Fiutowski³⁷ , F. Fleuret¹⁴ ,
 M. Fontana²² , F. Fontanelli^{26,l} , L. F. Foreman⁶⁰ , R. Forty⁴⁶ , D. Foulds-Holt⁵³ ,
 M. Franco Sevilla⁶⁴ , M. Frank⁴⁶ , E. Franzoso^{23,j} , G. Frau¹⁹ , C. Frei⁴⁶ ,
 D.A. Friday⁶⁰ , L. Frontini^{27,m} , J. Fu⁷ , Q. Fuehring¹⁷ , Y. Fujii¹ , T. Fulghesu¹⁵ ,
 E. Gabriel³⁵ , G. Galati^{21,g} , M.D. Galati³⁵ , A. Gallas Torreira⁴⁴ , D. Galli^{22,h} ,
 S. Gambetta^{56,46} , M. Gandelman³ , P. Gandini²⁷ , H. Gao⁷ , R. Gao⁶¹ , Y. Gao⁸ ,
 Y. Gao⁶ , Y. Gao⁸ , M. Garau^{29,i} , L.M. Garcia Martin⁴⁷ , P. Garcia Moreno⁴³ ,
 J. García Pardiñas⁴⁶ , B. Garcia Plana⁴⁴ , K. G. Garg⁸ , L. Garrido⁴³ , C. Gaspar⁴⁶ ,
 R.E. Geertsema³⁵ , L.L. Gerken¹⁷ , E. Gersabeck⁶⁰ , M. Gersabeck⁶⁰ , T. Gershon⁵⁴ ,
 Z. Ghorbanimoghaddam⁵² , L. Giambastiani³⁰ , F. I. Giasemis^{15,d} , V. Gibson⁵³ ,
 H.K. Giemza³⁹ , A.L. Gilman⁶¹ , M. Giovannetti²⁵ , A. Gioventù⁴³ ,
 P. Gironella Gironell⁴³ , C. Giugliano^{23,j} , M.A. Giza³⁸ , E.L. Gkoukousis⁵⁹ ,
 F.C. Glaser^{13,19} , V.V. Gligorov¹⁵ , C. Göbel⁶⁷ , E. Golobardes⁴² , D. Golubkov⁴¹ ,
 A. Golutvin^{59,41,46} , A. Gomes^{2,a,†} , S. Gomez Fernandez⁴³ , F. Goncalves Abrantes⁶¹ ,
 M. Goncerz³⁸ , G. Gong⁴ , J. A. Gooding¹⁷ , I.V. Gorelov⁴¹ , C. Gotti²⁸ ,
 J.P. Grabowski⁷³ , L.A. Granado Cardoso⁴⁶ , E. Graugés⁴³ , E. Graverini⁴⁷ ,
 L. Gazette⁵⁴ , G. Graziani , A. T. Grecu⁴⁰ , L.M. Greeven³⁵ , N.A. Grieser⁶³ ,
 L. Grillo⁵⁷ , S. Gromov⁴¹ , C. Gu¹⁴ , M. Guarise²³ , M. Guittiere¹³ , V. Guliaeva⁴¹ ,
 P. A. Günther¹⁹ , A.-K. Guseinov⁴¹ , E. Gushchin⁴¹ , Y. Guz^{6,41,46} , T. Gys⁴⁶ ,
 T. Hadavizadeh¹ , C. Hadjivasiliou⁶⁴ , G. Haefeli⁴⁷ , C. Haen⁴⁶ , J. Haimberger⁴⁶ ,
 M. Hajheidari⁴⁶ , T. Halewood-leagas⁵⁸ , M.M. Halvorsen⁴⁶ , P.M. Hamilton⁶⁴ ,
 J. Hammerich⁵⁸ , Q. Han⁸ , X. Han¹⁹ , S. Hansmann-Menzemer¹⁹ , L. Hao⁷ ,
 N. Harnew⁶¹ , T. Harrison⁵⁸ , M. Hartmann¹³ , C. Hasse⁴⁶ , J. He^{7,c} , K. Heijhoff³⁵ ,
 F. Hemmer⁴⁶ , C. Henderson⁶³ , R.D.L. Henderson^{1,54} , A.M. Hennequin⁴⁶ ,
 K. Hennessy⁵⁸ , L. Henry⁴⁷ , J. Herd⁵⁹ , J. Heuel¹⁶ , A. Hicheur³ , D. Hill⁴⁷ ,
 S.E. Hollitt¹⁷ , J. Horswill⁶⁰ , R. Hou⁸ , Y. Hou¹⁰ , N. Howarth⁵⁸ , J. Hu¹⁹ , J. Hu⁶⁹ ,
 W. Hu⁶ , X. Hu⁴ , W. Huang⁷ , W. Hulsbergen³⁵ , R.J. Hunter⁵⁴ , M. Hushchyn⁴¹ ,
 D. Hutchcroft⁵⁸ , M. Idzik³⁷ , D. Ilin⁴¹ , P. Ilten⁶³ , A. Inglessi⁴¹ , A. Iniukhin⁴¹ ,
 A. Ishteev⁴¹ , K. Ivshin⁴¹ , R. Jacobsson⁴⁶ , H. Jage¹⁶ , S.J. Jaimes Elles^{45,72} ,
 S. Jakobsen⁴⁶ , E. Jans³⁵ , B.K. Jashal⁴⁵ , A. Jawahery⁶⁴ , V. Jevtic¹⁷ , E. Jiang⁶⁴ ,
 X. Jiang^{5,7} , Y. Jiang⁷ , Y. J. Jiang⁶ , M. John⁶¹ , D. Johnson⁵¹ , C.R. Jones⁵³ ,
 T.P. Jones⁵⁴ , S. Joshi³⁹ , B. Jost⁴⁶ , N. Jurik⁴⁶ , I. Juszczak³⁸ , D. Kaminaris⁴⁷ ,
 S. Kandybei⁴⁹ , Y. Kang⁴ , M. Karacson⁴⁶ , D. Karpenkov⁴¹ , M. Karpov⁴¹ , A. M.
 Kauniskangas⁴⁷ , J.W. Kautz⁶³ , F. Keizer⁴⁶ , D.M. Keller⁶⁶ , M. Kenzie⁵³ ,
 T. Ketel³⁵ , B. Khanji⁶⁶ , A. Kharisova⁴¹ , S. Kholodenko³² , G. Khreich¹³ ,
 T. Kirn¹⁶ , V.S. Kirsebom⁴⁷ , O. Kitouni⁶² , S. Klaver³⁶ , N. Kleijne^{32,g} ,

K. Klimaszewski³⁹ , M.R. Kmiec³⁹ , S. Koliiev⁵⁰ , L. Kolk¹⁷ , A. Konoplyannikov⁴¹ ,
 P. Kopciwicz^{37,46} , P. Koppenburg³⁵ , M. Korolev⁴¹ , I. Kostiuik³⁵ , O. Kot⁵⁰,
 S. Kotriakhova , A. Kozachuk⁴¹ , P. Kravchenko⁴¹ , L. Kravchuk⁴¹ , M. Kreps⁵⁴ ,
 S. Kretzschmar¹⁶ , P. Krovovny⁴¹ , W. Krupa⁶⁶ , W. Krzemien³⁹ , J. Kubat¹⁹,
 S. Kubis⁷⁷ , W. Kucewicz³⁸ , M. Kucharczyk³⁸ , V. Kudryavtsev⁴¹ , E. Kulikova⁴¹ ,
 A. Kupsc⁷⁸ , B. K. Kutsenko¹² , D. Lacarrere⁴⁶ , G. Lafferty⁶⁰ , A. Lai²⁹ ,
 A. Lampis²⁹ , D. Lancierini⁴⁸ , C. Landesa Gomez⁴⁴ , J.J. Lane¹ , R. Lane⁵² ,
 C. Langenbruch¹⁹ , J. Langer¹⁷ , O. Lantwin⁴¹ , T. Latham⁵⁴ , F. Lazzari^{32,r} ,
 C. Lazzeroni⁵¹ , R. Le Gac¹² , S.H. Lee⁷⁹ , R. Lefèvre¹¹ , A. Leflat⁴¹ , S. Legotin⁴¹ ,
 M. Lehuraux⁵⁴ , O. Leroy¹² , T. Lesiak³⁸ , B. Leverington¹⁹ , A. Li⁴ , H. Li⁶⁹ ,
 K. Li⁸ , L. Li⁶⁰ , P. Li⁴⁶ , P.-R. Li⁷⁰ , S. Li⁸ , T. Li⁵ , T. Li⁶⁹ , Y. Li⁸, Y. Li⁵ ,
 Z. Li⁶⁶ , Z. Lian⁴ , X. Liang⁶⁶ , C. Lin⁷ , T. Lin⁵⁵ , R. Lindner⁴⁶ , V. Lisovskiy⁴⁷ ,
 R. Litvinov^{29,i} , G. Liu⁶⁹ , H. Liu⁷ , K. Liu⁷⁰ , Q. Liu⁷ , S. Liu^{5,7} , Y. Liu⁵⁶ ,
 Y. Liu⁷⁰, Y. L. Liu⁵⁹ , A. Lobo Salvia⁴³ , A. Loi²⁹ , J. Lomba Castro⁴⁴ , T. Long⁵³ ,
 J.H. Lopes³ , A. Lopez Huertas⁴³ , S. López Soliño⁴⁴ , G.H. Lovell⁵³ , C. Lucarelli^{24,k} ,
 D. Lucchesi^{30,o} , S. Luchuk⁴¹ , M. Lucio Martinez⁷⁶ , V. Lukashenko^{35,50} , Y. Luo⁴ ,
 A. Lupato³⁰ , E. Luppi^{23,j} , K. Lynch²⁰ , X.-R. Lyu⁷ , G. M. Ma⁴ , R. Ma⁷ ,
 S. Maccolini¹⁷ , F. Machefert¹³ , F. Maciuc⁴⁰ , I. Mackay⁶¹ , L.R. Madhan Mohan⁵³ ,
 M. M. Madurai⁵¹ , A. Maevskiy⁴¹ , D. Magdalinski³⁵ , D. Maisuzenko⁴¹ ,
 M.W. Majewski³⁷, J.J. Malczewski³⁸ , S. Malde⁶¹ , B. Malecki^{38,46} , L. Malentacca⁴⁶,
 A. Malinin⁴¹ , T. Maltsev⁴¹ , G. Manca^{29,i} , G. Mancinelli¹² , C. Mancuso^{27,13,m} ,
 R. Manera Escalero⁴³, D. Manuzzi²² , D. Marangotto^{27,m} , J.F. Marchand¹⁰ ,
 R. Marchevski⁴⁷ , U. Marconi²² , S. Mariani⁴⁶ , C. Marin Benito^{43,46} , J. Marks¹⁹ ,
 A.M. Marshall⁵² , P.J. Marshall⁵⁸, G. Martelli^{31,p} , G. Martellotti³³ , L. Martinazzoli⁴⁶ ,
 M. Martinelli^{28,n} , D. Martinez Santos⁴⁴ , F. Martinez Vidal⁴⁵ , A. Massafferri² ,
 M. Materok¹⁶ , R. Matev⁴⁶ , A. Mathad⁴⁸ , V. Matiunin⁴¹ , C. Matteuzzi^{66,28} ,
 K.R. Mattioli¹⁴ , A. Mauri⁵⁹ , E. Maurice¹⁴ , J. Mauricio⁴³ , M. Mazurek⁴⁶ ,
 M. McCann⁵⁹ , L. McConnell²⁰ , T.H. McGrath⁶⁰ , N.T. McHugh⁵⁷ , A. McNab⁶⁰ ,
 R. McNulty²⁰ , B. Meadows⁶³ , G. Meier¹⁷ , D. Melnychuk³⁹ , M. Merk^{35,76} ,
 A. Merli^{27,m} , L. Meyer Garcia³ , D. Miao^{5,7} , H. Miao⁷ , M. Mikhasenko^{73,e} ,
 D.A. Milanese⁷² , A. Minotti^{28,n} , E. Minucci⁶⁶ , T. Miralles¹¹ , S.E. Mitchell⁵⁶ ,
 B. Mitreska¹⁷ , D.S. Mitzel¹⁷ , A. Modak⁵⁵ , A. Mödden ¹⁷ , R.A. Mohammed⁶¹ ,
 R.D. Moise¹⁶ , S. Mokhnenko⁴¹ , T. Mombächer⁴⁶ , M. Monk^{54,1} , I.A. Monroy⁷² ,
 S. Monteil¹¹ , A. Morcillo Gomez⁴⁴ , G. Morello²⁵ , M.J. Morello^{32,q} ,
 M.P. Morgenthaler¹⁹ , J. Moron³⁷ , A.B. Morris⁴⁶ , A.G. Morris¹² , R. Mountain⁶⁶ ,
 H. Mu⁴ , Z. M. Mu⁶ , E. Muhammad⁵⁴ , F. Muheim⁵⁶ , M. Mulder⁷⁵ , K. Müller⁴⁸ ,
 F. Muñoz-Rojas⁹ , R. Murta⁵⁹ , P. Naik⁵⁸ , T. Nakada⁴⁷ , R. Nandakumar⁵⁵ ,
 T. Nanut⁴⁶ , I. Nasteva³ , M. Needham⁵⁶ , N. Neri^{27,m} , S. Neubert⁷³ , N. Neufeld⁴⁶ ,
 P. Neustroev⁴¹, R. Newcombe⁵⁹, J. Nicolini^{17,13} , D. Nicotra⁷⁶ , E.M. Niel⁴⁷ ,
 N. Nikitin⁴¹ , P. Nogga⁷³, N.S. Nolte⁶² , C. Normand^{10,i,29} , J. Novoa Fernandez⁴⁴ ,
 G. Nowak⁶³ , C. Nunez⁷⁹ , H. N. Nur⁵⁷ , A. Oblakowska-Mucha³⁷ , V. Obraztsov⁴¹ ,
 T. Oeser¹⁶ , S. Okamura^{23,j,46} , R. Oldeman^{29,i} , F. Oliva⁵⁶ , M. Olocco¹⁷ ,
 C.J.G. Onderwater⁷⁶ , R.H. O'Neil⁵⁶ , J.M. Otalora Goicochea³ , T. Ovsiannikova⁴¹ ,
 P. Owen⁴⁸ , A. Oyanguren⁴⁵ , O. Ozcelik⁵⁶ , K.O. Padeken⁷³ , B. Pagare⁵⁴ ,
 P.R. Pais¹⁹ , T. Pajero⁶¹ , A. Palano²¹ , M. Palutan²⁵ , G. Panshin⁴¹ , L. Paolucci⁵⁴ ,
 A. Papanestis⁵⁵ , M. Pappagallo^{21,g} , L.L. Pappalardo^{23,j} , C. Pappenheimer⁶³ ,
 C. Parkes⁶⁰ , B. Passalacqua^{23,j} , G. Passaleva²⁴ , D. Passaro^{32,q} , A. Pastore²¹ ,
 M. Patel⁵⁹ , J. Patoc⁶¹ , C. Patrignani^{22,h} , C.J. Pawley⁷⁶ , A. Pellegrino³⁵ ,
 M. Pepe Altarelli²⁵ , S. Perazzini²² , D. Pereima⁴¹ , A. Pereiro Castro⁴⁴ , P. Perret¹¹ ,
 A. Perro⁴⁶ , K. Petridis⁵² , A. Petrolini^{26,l} , S. Petrucci⁵⁶ , H. Pham⁶⁶ , L. Pica^{32,q} 

M. Piccini³¹ , B. Pietrzyk¹⁰ , G. Pietrzyk¹³ , D. Pinci³³ , F. Pisani⁴⁶ ,
M. Pizzichemi^{28,n} , V. Placinta⁴⁰ , M. Plo Casasus⁴⁴ , F. Polci^{15,46} , M. Poli Lener²⁵ ,
A. Poluektov¹² , N. Polukhina⁴¹ , I. Polyakov⁴⁶ , E. Polycarpo³ , S. Ponce⁴⁶ ,
D. Popov⁷ , S. Poslavskii⁴¹ , K. Prasanth³⁸ , L. Promberger¹⁹ , C. Prouve⁴⁴ ,
V. Pugatch⁵⁰ , V. Puill¹³ , G. Punzi^{32,r} , H.R. Qi⁴ , W. Qian⁷ , N. Qin⁴ , S. Qu⁴ ,
R. Quagliani⁴⁷ , B. Rachwal³⁷ , J.H. Rademacker⁵² , M. Rama³² , M.
Ramírez García⁷⁹ , M. Ramos Pernas⁵⁴ , M.S. Rangel³ , F. Ratnikov⁴¹ , G. Raven³⁶ ,
M. Rebollo De Miguel⁴⁵ , F. Redi⁴⁶ , J. Reich⁵² , F. Reiss⁶⁰ , Z. Ren⁴ ,
P.K. Resmi⁶¹ , R. Ribatti^{32,q} , G. R. Ricart^{14,80} , D. Riccardi^{32,q} , S. Ricciardi⁵⁵ ,
K. Richardson⁶² , M. Richardson-Slipper⁵⁶ , K. Rinnert⁵⁸ , P. Robbe¹³ ,
G. Robertson⁵⁶ , E. Rodrigues^{58,46} , E. Rodriguez Fernandez⁴⁴ ,
J.A. Rodriguez Lopez⁷² , E. Rodriguez Rodriguez⁴⁴ , A. Rogovskiy⁵⁵ , D.L. Rolf⁴⁶ ,
A. Rollings⁶¹ , P. Roloff⁴⁶ , V. Romanovskiy⁴¹ , M. Romero Lamas⁴⁴ ,
A. Romero Vidal⁴⁴ , G. Romolini²³ , F. Ronchetti⁴⁷ , M. Rotondo²⁵ , S. R. Roy¹⁹ ,
M.S. Rudolph⁶⁶ , T. Ruf⁴⁶ , M. Ruiz Diaz¹⁹ , R.A. Ruiz Fernandez⁴⁴ ,
J. Ruiz Vidal^{78,y} , A. Ryzhikov⁴¹ , J. Ryzka³⁷ , J.J. Saborido Silva⁴⁴ , R. Sadek¹⁴ ,
N. Sagidova⁴¹ , N. Sahoo⁵¹ , B. Saitta^{29,i} , M. Salomoni⁴⁶ , C. Sanchez Gras³⁵ ,
I. Sanderswood⁴⁵ , R. Santacesaria³³ , C. Santamarina Rios⁴⁴ , M. Santimaria²⁵ ,
L. Santoro² , E. Santovetti³⁴ , A. Saputi^{23,46} , D. Saranin⁴¹ , G. Sarpis⁵⁶ ,
M. Sarpis⁷³ , A. Sarti³³ , C. Satriano^{33,s} , A. Satta³⁴ , M. Saur⁶ , D. Savrina⁴¹ ,
H. Sazak¹¹ , L.G. Scantlebury Smead⁶¹ , A. Scarabotto¹⁵ , S. Schael¹⁶ , S. Scherl⁵⁸ , A.
M. Schertz⁷⁴ , M. Schiller⁵⁷ , H. Schindler⁴⁶ , M. Schmelling¹⁸ , B. Schmidt⁴⁶ ,
S. Schmitt¹⁶ , H. Schmitz⁷³ , O. Schneider⁴⁷ , A. Schopper⁴⁶ , N. Schulte¹⁷ ,
S. Schulte⁴⁷ , M.H. Schune¹³ , R. Schwemmer⁴⁶ , G. Schwering¹⁶ , B. Sciascia²⁵ ,
A. Sciuccati⁴⁶ , S. Sellam⁴⁴ , A. Semennikov⁴¹ , M. Senghi Soares³⁶ , A. Sergi^{26,l} ,
N. Serra^{48,46} , L. Sestini³⁰ , A. Seuthe¹⁷ , Y. Shang⁶ , D.M. Shangase⁷⁹ ,
M. Shapkin⁴¹ , I. Shchemerov⁴¹ , L. Shchutska⁴⁷ , T. Shears⁵⁸ , L. Shekhtman⁴¹ ,
Z. Shen⁶ , S. Sheng^{5,7} , V. Shevchenko⁴¹ , B. Shi⁷ , E.B. Shields^{28,n} , Y. Shimizu¹³ ,
E. Shmanin⁴¹ , R. Shorkin⁴¹ , J.D. Shupperd⁶⁶ , R. Silva Coutinho⁶⁶ , G. Simi³⁰ ,
S. Simone^{21,g} , N. Skidmore⁶⁰ , R. Skuza¹⁹ , T. Skwarnicki⁶⁶ , M.W. Slater⁵¹ ,
J.C. Smallwood⁶¹ , E. Smith⁶² , K. Smith⁶⁵ , M. Smith⁵⁹ , A. Snoch³⁵ ,
L. Soares Lavra⁵⁶ , M.D. Sokoloff⁶³ , F.J.P. Soler⁵⁷ , A. Solomin^{41,52} , A. Solovev⁴¹ ,
I. Solovyev⁴¹ , R. Song¹ , Y. Song⁴⁷ , Y. Song⁴ , Y. S. Song⁶ ,
F.L. Souza De Almeida³ , B. Souza De Paula³ , E. Spadaro Norella^{27,m} , E. Spedicato²² ,
J.G. Speer¹⁷ , E. Spiridenkov⁴¹ , P. Spradlin⁵⁷ , V. Sriskaran⁴⁶ , F. Stagni⁴⁶ ,
M. Stahl⁴⁶ , S. Stahl⁴⁶ , S. Stanislaus⁶¹ , E.N. Stein⁴⁶ , O. Steinkamp⁴⁸ ,
O. Stenyakin⁴¹ , H. Stevens¹⁷ , D. Strekalina⁴¹ , Y. Su⁷ , F. Suljik⁶¹ , J. Sun²⁹ ,
L. Sun⁷¹ , Y. Sun⁶⁴ , P.N. Swallow⁵¹ , K. Swientek³⁷ , F. Swystun⁵⁴ , A. Szabelski³⁹ ,
T. Szumlak³⁷ , M. Szymanski⁴⁶ , Y. Tan⁴ , S. Taneja⁶⁰ , M.D. Tat⁶¹ , A. Terentev⁴⁸ ,
F. Terzuoli^{32,u} , F. Teubert⁴⁶ , E. Thomas⁴⁶ , D.J.D. Thompson⁵¹ , H. Tilquin⁵⁹ ,
V. Tisserand¹¹ , S. T'Jampens¹⁰ , M. Tobin⁵ , L. Tomassetti^{23,j} , G. Tonani^{27,m} ,
X. Tong⁶ , D. Torres Machado² , L. Toscano¹⁷ , D.Y. Tou⁴ , C. Trippi⁴² , G. Tuci¹⁹ ,
N. Tuning³⁵ , L.H. Uecker¹⁹ , A. Ukleja³⁷ , D.J. Unverzagt¹⁹ , E. Ursov⁴¹ ,
A. Usachov³⁶ , A. Ustyuzhanin⁴¹ , U. Uwer¹⁹ , V. Vagnoni²² , A. Valassi⁴⁶ ,
G. Valenti²² , N. Valls Canudas⁴² , H. Van Hecke⁶⁵ , E. van Herwijnen⁵⁹ ,
C.B. Van Hulse^{44,w} , R. Van Laak⁴⁷ , M. van Veghel³⁵ , R. Vazquez Gomez⁴³ ,
P. Vazquez Regueiro⁴⁴ , C. Vázquez Sierra⁴⁴ , S. Vecchi²³ , J.J. Velthuis⁵² ,
M. Veltri^{24,v} , A. Venkateswaran⁴⁷ , M. Vesterinen⁵⁴ , D. Vieira⁶³ , M. Vieites Diaz⁴⁶ ,
X. Vilasis-Cardona⁴² , E. Vilella Figueras⁵⁸ , A. Villa²² , P. Vincent¹⁵ , F.C. Volle¹³ ,
D. vom Bruch¹² , V. Vorobyev⁴¹ , N. Voropaev⁴¹ , K. Vos⁷⁶ , C. Vrahas⁵⁶ , J. Walsh³² ,

E.J. Walton¹ , G. Wan⁶ , C. Wang¹⁹ , G. Wang⁸ , J. Wang⁶ , J. Wang⁵ , J. Wang⁴ , J. Wang⁷¹ , M. Wang²⁷ , N. W. Wang⁷ , R. Wang⁵² , X. Wang⁶⁹ , X. W. Wang⁵⁹ , Y. Wang⁸ , Z. Wang¹³ , Z. Wang⁴ , Z. Wang⁷ , J.A. Ward^{54,1} , N.K. Watson⁵¹ , D. Websdale⁵⁹ , Y. Wei⁶ , B.D.C. Westhenry⁵² , D.J. White⁶⁰ , M. Whitehead⁵⁷ , A.R. Wiederhold⁵⁴ , D. Wiedner¹⁷ , G. Wilkinson⁶¹ , M.K. Wilkinson⁶³ , M. Williams⁶² , M.R.J. Williams⁵⁶ , R. Williams⁵³ , F.F. Wilson⁵⁵ , W. Wislicki³⁹ , M. Witek³⁸ , L. Witola¹⁹ , C.P. Wong⁶⁵ , G. Wormser¹³ , S.A. Wotton⁵³ , H. Wu⁶⁶ , J. Wu⁸ , Y. Wu⁶ , K. Wyllie⁴⁶ , S. Xian⁶⁹ , Z. Xiang⁵ , Y. Xie⁸ , A. Xu³² , J. Xu⁷ , L. Xu⁴ , L. Xu⁴ , M. Xu⁵⁴ , Z. Xu¹¹ , Z. Xu⁷ , Z. Xu⁵ , D. Yang⁴ , S. Yang⁷ , X. Yang⁶ , Y. Yang^{26,l} , Z. Yang⁶ , Z. Yang⁶⁴ , V. Yeroshenko¹³ , H. Yeung⁶⁰ , H. Yin⁸ , C. Y. Yu⁶ , J. Yu⁶⁸ , X. Yuan⁵ , E. Zaffaroni⁴⁷ , M. Zavertyaev¹⁸ , M. Zdybal³⁸ , M. Zeng⁴ , C. Zhang⁶ , D. Zhang⁸ , J. Zhang⁷ , L. Zhang⁴ , S. Zhang⁶⁸ , S. Zhang⁶ , Y. Zhang⁶ , Y. Zhang⁶¹ , Y. Z. Zhang⁴ , Y. Zhao¹⁹ , A. Zharkova⁴¹ , A. Zhelezov¹⁹ , X. Z. Zheng⁴ , Y. Zheng⁷ , T. Zhou⁶ , X. Zhou⁸ , Y. Zhou⁷ , V. Zhovkovska¹³ , L. Z. Zhu⁷ , X. Zhu⁴ , X. Zhu⁸ , Z. Zhu⁷ , V. Zhukov^{16,41} , J. Zhuo⁴⁵ , Q. Zou^{5,7} , D. Zuliani³⁰ , G. Zunica⁶⁰ .

¹*School of Physics and Astronomy, Monash University, Melbourne, Australia*

²*Centro Brasileiro de Pesquisas Físicas (CBPF), Rio de Janeiro, Brazil*

³*Universidade Federal do Rio de Janeiro (UFRJ), Rio de Janeiro, Brazil*

⁴*Center for High Energy Physics, Tsinghua University, Beijing, China*

⁵*Institute Of High Energy Physics (IHEP), Beijing, China*

⁶*School of Physics State Key Laboratory of Nuclear Physics and Technology, Peking University, Beijing, China*

⁷*University of Chinese Academy of Sciences, Beijing, China*

⁸*Institute of Particle Physics, Central China Normal University, Wuhan, Hubei, China*

⁹*Consejo Nacional de Rectores (CONARE), San Jose, Costa Rica*

¹⁰*Université Savoie Mont Blanc, CNRS, IN2P3-LAPP, Annecy, France*

¹¹*Université Clermont Auvergne, CNRS/IN2P3, LPC, Clermont-Ferrand, France*

¹²*Aix Marseille Univ, CNRS/IN2P3, CPPM, Marseille, France*

¹³*Université Paris-Saclay, CNRS/IN2P3, IJCLab, Orsay, France*

¹⁴*Laboratoire Leprince-Ringuet, CNRS/IN2P3, Ecole Polytechnique, Institut Polytechnique de Paris, Palaiseau, France*

¹⁵*LPNHE, Sorbonne Université, Paris Diderot Sorbonne Paris Cité, CNRS/IN2P3, Paris, France*

¹⁶*I. Physikalisches Institut, RWTH Aachen University, Aachen, Germany*

¹⁷*Fakultät Physik, Technische Universität Dortmund, Dortmund, Germany*

¹⁸*Max-Planck-Institut für Kernphysik (MPIK), Heidelberg, Germany*

¹⁹*Physikalisches Institut, Ruprecht-Karls-Universität Heidelberg, Heidelberg, Germany*

²⁰*School of Physics, University College Dublin, Dublin, Ireland*

²¹*INFN Sezione di Bari, Bari, Italy*

²²*INFN Sezione di Bologna, Bologna, Italy*

²³*INFN Sezione di Ferrara, Ferrara, Italy*

²⁴*INFN Sezione di Firenze, Firenze, Italy*

²⁵*INFN Laboratori Nazionali di Frascati, Frascati, Italy*

²⁶*INFN Sezione di Genova, Genova, Italy*

²⁷*INFN Sezione di Milano, Milano, Italy*

²⁸*INFN Sezione di Milano-Bicocca, Milano, Italy*

²⁹*INFN Sezione di Cagliari, Monserrato, Italy*

³⁰*Università degli Studi di Padova, Università e INFN, Padova, Padova, Italy*

³¹*INFN Sezione di Perugia, Perugia, Italy*

³²*INFN Sezione di Pisa, Pisa, Italy*

³³*INFN Sezione di Roma La Sapienza, Roma, Italy*

³⁴*INFN Sezione di Roma Tor Vergata, Roma, Italy*

³⁵*Nikhef National Institute for Subatomic Physics, Amsterdam, Netherlands*

³⁶*Nikhef National Institute for Subatomic Physics and VU University Amsterdam, Amsterdam,*

Netherlands

- ³⁷ AGH - University of Science and Technology, Faculty of Physics and Applied Computer Science, Kraków, Poland
- ³⁸ Henryk Niewodniczanski Institute of Nuclear Physics Polish Academy of Sciences, Kraków, Poland
- ³⁹ National Center for Nuclear Research (NCBJ), Warsaw, Poland
- ⁴⁰ Horia Hulubei National Institute of Physics and Nuclear Engineering, Bucharest-Magurele, Romania
- ⁴¹ Affiliated with an institute covered by a cooperation agreement with CERN
- ⁴² DS4DS, La Salle, Universitat Ramon Llull, Barcelona, Spain
- ⁴³ ICCUB, Universitat de Barcelona, Barcelona, Spain
- ⁴⁴ Instituto Galego de Física de Altas Enerxías (IGFAE), Universidade de Santiago de Compostela, Santiago de Compostela, Spain
- ⁴⁵ Instituto de Física Corpuscular, Centro Mixto Universidad de Valencia - CSIC, Valencia, Spain
- ⁴⁶ European Organization for Nuclear Research (CERN), Geneva, Switzerland
- ⁴⁷ Institute of Physics, Ecole Polytechnique Fédérale de Lausanne (EPFL), Lausanne, Switzerland
- ⁴⁸ Physik-Institut, Universität Zürich, Zürich, Switzerland
- ⁴⁹ NSC Kharkiv Institute of Physics and Technology (NSC KIPT), Kharkiv, Ukraine
- ⁵⁰ Institute for Nuclear Research of the National Academy of Sciences (KINR), Kyiv, Ukraine
- ⁵¹ University of Birmingham, Birmingham, United Kingdom
- ⁵² H.H. Wills Physics Laboratory, University of Bristol, Bristol, United Kingdom
- ⁵³ Cavendish Laboratory, University of Cambridge, Cambridge, United Kingdom
- ⁵⁴ Department of Physics, University of Warwick, Coventry, United Kingdom
- ⁵⁵ STFC Rutherford Appleton Laboratory, Didcot, United Kingdom
- ⁵⁶ School of Physics and Astronomy, University of Edinburgh, Edinburgh, United Kingdom
- ⁵⁷ School of Physics and Astronomy, University of Glasgow, Glasgow, United Kingdom
- ⁵⁸ Oliver Lodge Laboratory, University of Liverpool, Liverpool, United Kingdom
- ⁵⁹ Imperial College London, London, United Kingdom
- ⁶⁰ Department of Physics and Astronomy, University of Manchester, Manchester, United Kingdom
- ⁶¹ Department of Physics, University of Oxford, Oxford, United Kingdom
- ⁶² Massachusetts Institute of Technology, Cambridge, MA, United States
- ⁶³ University of Cincinnati, Cincinnati, OH, United States
- ⁶⁴ University of Maryland, College Park, MD, United States
- ⁶⁵ Los Alamos National Laboratory (LANL), Los Alamos, NM, United States
- ⁶⁶ Syracuse University, Syracuse, NY, United States
- ⁶⁷ Pontifícia Universidade Católica do Rio de Janeiro (PUC-Rio), Rio de Janeiro, Brazil, associated to ³
- ⁶⁸ School of Physics and Electronics, Hunan University, Changsha City, China, associated to ⁸
- ⁶⁹ Guangdong Provincial Key Laboratory of Nuclear Science, Guangdong-Hong Kong Joint Laboratory of Quantum Matter, Institute of Quantum Matter, South China Normal University, Guangzhou, China, associated to ⁴
- ⁷⁰ Lanzhou University, Lanzhou, China, associated to ⁵
- ⁷¹ School of Physics and Technology, Wuhan University, Wuhan, China, associated to ⁴
- ⁷² Departamento de Física, Universidad Nacional de Colombia, Bogota, Colombia, associated to ¹⁵
- ⁷³ Universität Bonn - Helmholtz-Institut für Strahlen und Kernphysik, Bonn, Germany, associated to ¹⁹
- ⁷⁴ Eotvos Lorand University, Budapest, Hungary, associated to ⁴⁶
- ⁷⁵ Van Swinderen Institute, University of Groningen, Groningen, Netherlands, associated to ³⁵
- ⁷⁶ Universiteit Maastricht, Maastricht, Netherlands, associated to ³⁵
- ⁷⁷ Tadeusz Kosciuszko Cracow University of Technology, Cracow, Poland, associated to ³⁸
- ⁷⁸ Department of Physics and Astronomy, Uppsala University, Uppsala, Sweden, associated to ⁵⁷
- ⁷⁹ University of Michigan, Ann Arbor, MI, United States, associated to ⁶⁶
- ⁸⁰ Departement de Physique Nucleaire (SPhN), Gif-Sur-Yvette, France

^a Universidade de Brasília, Brasília, Brazil

^b Centro Federal de Educação Tecnológica Celso Suckow da Fonseca, Rio De Janeiro, Brazil

^c Hangzhou Institute for Advanced Study, UCAS, Hangzhou, China

^d LIP6, Sorbonne Université, Paris, France

^e Excellence Cluster ORIGINS, Munich, Germany

^f Universidad Nacional Autónoma de Honduras, Tegucigalpa, Honduras

^g Università di Bari, Bari, Italy

- ^h *Università di Bologna, Bologna, Italy*
ⁱ *Università di Cagliari, Cagliari, Italy*
^j *Università di Ferrara, Ferrara, Italy*
^k *Università di Firenze, Firenze, Italy*
^l *Università di Genova, Genova, Italy*
^m *Università degli Studi di Milano, Milano, Italy*
ⁿ *Università di Milano Bicocca, Milano, Italy*
^o *Università di Padova, Padova, Italy*
^p *Università di Perugia, Perugia, Italy*
^q *Scuola Normale Superiore, Pisa, Italy*
^r *Università di Pisa, Pisa, Italy*
^s *Università della Basilicata, Potenza, Italy*
^t *Università di Roma Tor Vergata, Roma, Italy*
^u *Università di Siena, Siena, Italy*
^v *Università di Urbino, Urbino, Italy*
^w *Universidad de Alcalá, Alcalá de Henares , Spain*
^x *Universidade da Coruña, Coruña, Spain*
^y *Department of Physics/Division of Particle Physics, Lund, Sweden*
[†] *Deceased*